IEEE Access
Multidisciplinary | Rapid Review | Open Access Journal

Received October 8, 2019, accepted November 11, 2019, date of publication November 21, 2019, date of current version December 6, 2019.

Digital Object Identifier 10.1109/ACCESS.2019.2955026

Effects of Multiple Semiconducting Screens on Line Parameters and Wave Properties of Underground Cable

SWARNANKUR GHOSH[1], MOUSAM GHOSH[2], (Member, IEEE), AND SUPRIYO DAS[1], (Member, IEEE)

[1]Department of Electrical Engineering, National Institute of Technology Meghalaya, Shillong 793003, India
[2]Electrical Engineering Department, Ramkrishna Mahato Government Engineering College, Narayanpur 723201, India

Corresponding author: Swarnankur Ghosh (swarnankur.ghosh@nitm.ac.in)

ABSTRACT Along with the geometric and electromagnetic properties, incorporation of multiple semiconducting screens in an underground (UG) power cable influences the primary line parameters as well as wave properties of the cable. The impacts of multiple semiconducting screens in UG cable structure compared to the cable with single and without semiconducting screen have been reported in this paper. The effective impedance of conductor-semiconductor assembly in cable structure is determined based on the electromagnetic theory of tubular conductor. Further, the complete impedance matrix of the UG cable with multiple semiconducting screens is determined in both mesh and phase domain and reported in this paper. The expressions of the impedances of UG cable with multiple semiconducting screens as obtained using the electromagnetic approach also have been reproduced using the conventional loop current method to justify the robustness and accuracy of the adopted approach. Comparative analyses of various line parameters and wave properties between UG cables with multiple, single and without semiconducting screens have been carried out by varying the frequency as well as semiconducting screen properties. Such analyses indicate that the inclusion of multiple semiconducting screens can lead to the improvement in wave properties of UG cable in high frequency zone.

INDEX TERMS Attenuation, loop current, phase constant, phase domain, semiconductor, skin depth, double layered conductor.

I. INTRODUCTION

The wave propagation characteristics of underground cable are governed by the cable line parameters which are the function of cable geometric and electromagnetic properties. Therefore the inclusion of semiconducting screen in cable structure has considerable impact on cable line parameters, which in turn influences the wave properties of the cable. The line parameters as well as wave properties of the cable are derived from the expressions of cable impedance and admittance. After several attempts [1]–[4], the complete model of impedance and admittance of multilayered cable was first developed in [5] based on the electromagnetic theory of coaxial cylindrical conductor [6]. This model has found widespread application to accurately calculate the line parameters of the cable to study its wave properties as well as to develop cable routines of several commercial software like EMTP for transient study [7]–[12]. However, this model is mainly designated for a specific cable structure containing alternate conducting and insulating layers [5]. But most of the practical cable uses semiconducting screen between conducting and insulating layers, which has considerable effects on cable primary line parameters as well as wave propagation characteristics [13]–[15]. Thus it called for a modification in the existing model of cable impedance and admittance [5] to include the effect of the semiconducting screen. Initially, the effect of the semiconducting screen was either neglected [13], [14] or considered only in the expressions of shunt admittance of the cable [15]–[17]. Also, different numerical methods such as FEM and FDTD [18], [19], sub-conductor method [20]–[22] etc. were applied to calculate line parameters of the cable with semiconducting screen.

The associate editor coordinating the review of this manuscript and approving it for publication was Kuang Zhang.

But none of the above mentioned works was able to provide the explicit formulation of cable impedance in which the effect of the semiconducting screen was considered. The main constraint was that the conducting and semiconducting layer in cable structure with no insulation between them constituted a double layered conductor system whose closed form expressions of impedance was not available at that time. Finally, a mathematical model was developed in [23] to calculate the effective surface and mutual impedance of double layered conductor system by solving Maxwell's equations and applied successfully to modify the existing cable impedance model of [5] to incorporate the effect of semiconductor screen present in cable structure. This model was later verified using circuit analysis in [24]. Generally, more than one semiconducting screen is present in practical cable structure. However, the detail comparative analysis of the possible effects brought by introducing multiple semiconducting screens over a single semiconducting screen in cable structure was not done in [23]–[25]. Many subsequent works considered cable with more than one semiconducting screen as a test cable, but instead of exploring the effect of multiple semiconducting screens, they confined their attention to the determination of the effect of materialistic properties of the semiconductor on different high frequency phenomenon and wave propagation characteristics in UG cable [26]–[34]. Some works adopted different numerical methods like FEM or methods of moment (MOM) [35]–[38] or used conventional relationships [39] to study wave propagation through the cable containing semiconducting screen but refrain from discussing the effect of multiple semiconducting screens explicitly.

In this context, this paper attempts to present a complete analysis to determine the effect of introducing multiple semiconducting screens in cable structure on primary line parameters and wave properties of the cable. Here the effective surface and mutual impedance of conductor-semiconductor assembly present in cable structure are derived based on 'Schelkunoff's theory' of tubular conductor system. Based on these expressions, the complete impedance and admittance matrix of the cable with multiple semiconducting screens is determined in both mesh and phase domain. The same expressions of impedance of the cable with multiple semiconducting screens are reproduced using the conventional loop current method of circuit analysis to show the robustness and accuracy of the adopted electromagnetic approach of determining impedances of the cable. A comparative analysis on the effect of the variation of different electrical and geometric properties of the semiconducting screen on line parameters as well as the wave propagation characteristics of the cable with multiple, single and without semiconducting screen is performed over a wide range of frequency. This study shows explicitly that the introduction of multiple semiconducting screens in cable structure improves the wave propagation characteristics of the cable considerably compared to that of the cable with single and without semiconducting screen, especially at high frequency.

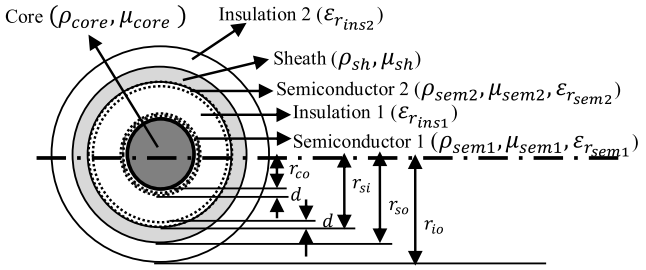

FIGURE 1. Cable with multiple semiconductors.

II. CABLE IMPEDANCE & ADMITTANCE

Consider a multilayer single core (SC) co-axial cable containing multiple semiconducting screens, one each on the core outer surface as well as sheath inner surface, as shown in Fig. 1. It is clear from Fig. 1 that each conducting and semiconducting layer resembles an individual coaxial tubular conductor. The surface and mutual impedance of such tubular conductor, which will be called component impedances throughout this paper unless stated otherwise, are determined from [6] as discussed in the next section.

A. IMPEDANCE OF TUBULAR CONDUCTOR

The relationship between longitudinal electric field and component current along the outer and inner surface of the tubular conductor was shown in [6] as follows,

$$E_{z_{in}} = I_{in}Z_{in} + I_{out}Z_m \tag{1}$$

$$E_{z_{out}} = I_{in}Z_m + I_{out}Z_{in} \tag{2}$$

where $E_{z_{in}}, E_{z_{out}}$ and I_{in}, I_{out} are respectively the longitudinal electric field intensity and currents along the inner and outer surface of the tubular conductor. The relationships depicted in (1) and (2) are stated as 'Schelkunoff's theorem 1 and 2' respectively. Based on this theorem, the expressions of following component impedances of the tubular conductor are obtained,

Z_{in} = Inner surface impedance of the cylindrical conductor

$$= \frac{m\rho_c}{2\pi r_{in} D}\{I_0(mr_{in})K_1(mr_{out}) + K_0(mr_{in})I_1(mr_{out})\} \tag{3}$$

Z_{out} = Outer surface impedance of the cylindrical conductor

$$= \frac{m\rho_c}{2\pi r_{out} D}\{I_0(mr_{out})K_1(mr_{in}) + K_0(mr_{out})I_1(mr_{in})\} \tag{4}$$

Z_m = Mutual impedance between inner and outer surfaces

$$= \frac{\rho_c}{2\pi r_{out} r_{in} D} \tag{5}$$

where,

$$D = \{I_1(mr_{out})K_1(mr_{in}) - K_1(mr_{out})I_1(mr_{in})\}$$

$$m = \sqrt{\frac{j\omega\mu_c}{\rho_c}} = \text{Reciprocal of skin depth}$$

ρ_c and μ_c are the resistivity and permeability of the cylindrical conductor, respectively.

r_{in} and r_{out} are the inner and outer radius respectively of the cylindrical conductor.

I_0, I_1, K_0 and K_1 are the modified Bessel's functions.

Based on (3) to (5), the surface and mutual impedance of each conducting and semiconducting screen present in the cable considered here are calculated.

B. IMPEDANCE OF CABLE WITHOUT SEMICONDUCTOR

If the single core multilayered coaxial cable, shown in *Fig.1*, is considered without semiconducting screen, then it will have alternate conducting and insulating layers whose complete impedance matrix ($[Z]_{mesh}$) can be derived in mesh domain based on [5], as follows,

$$[Z]_{mesh} = \begin{bmatrix} Z_{l_{11}} & Z_{l_{12}} \\ Z_{l_{21}} & Z_{l_{22}} \end{bmatrix} \tag{6}$$

where,

$Z_{l_{11}}$ = Self impedance of internal loop between core and sheath

$$= \mathfrak{Z}_{core_{out}} + \mathfrak{Z}_{sh_{in}} + \mathfrak{Z}_{ins_{12}} \tag{6a}$$

$Z_{l_{12}}$ = Mutual impedance of loop between core and sheath due to core current

$= Z_{l_{21}}$ = Mutual impedance of loop between core and sheath due to sheath current

$$= -\mathfrak{Z}_{sh_m} \tag{6b}$$

$Z_{l_{22}}$ = Self impedance of internal loop between sheath and earth

$$= \mathfrak{Z}_{sh_{out}} + Z_e + \mathfrak{Z}_{ins_{2e}} \tag{6c}$$

where,

$\mathfrak{Z}_{core_{out}}$ is the per unit length outer surface impedance of the core.

$\mathfrak{Z}_{sh_{in}}$ and $\mathfrak{Z}_{sh_{out}}$ are the per unit length component impedance of outer and inner surface of the sheath respectively.

$\mathfrak{Z}_{sh_m}$ is the per unit length mutual impedance between the inner and outer surface of the sheath.

All of the above mentioned component impedances can be determined using (3) to (5).

Z_e = Earth return impedance whose expression can be determined from [5].

$\mathfrak{Z}_{ins_{12}}$ and $\mathfrak{Z}_{ins_{2e}}$ are the impedance of insulation between core and sheath and sheath and earth respectively, given by $j\omega\frac{\mu_0}{2\pi}\ln\frac{r_{ins_{out}}}{r_{ins_{in}}}$ where $r_{ins_{in}}$ and $r_{ins_{out}}$ are respectively the inner and outer radius of the insulating layer.

C. IMPEDANCE OF CABLE WITH SEMICONDUCTING SCREEN

1) DERIVATION OF IMPEDANCE USING SCHELK-UNOFF'S THEOREM

The conducting and semiconducting layer in the SC cable shown in Fig. 1 with no insulation between them forms a double layered conductor system. To find the complete impedance of the cable with semiconducting screen, the impedance of the double layered conductor is needed to be determined first. Fig. 2 (a) and (b) show the cross sectional and longitudinal view respectively of a double layered conductor. The electric and magnetic properties of each constituent conducting layer are different, as shown in Fig. 2. From Fig. 2, it is clear that the double layered conductor system resembles a tubular conductor as a whole which is assumed to have the following component impedances,

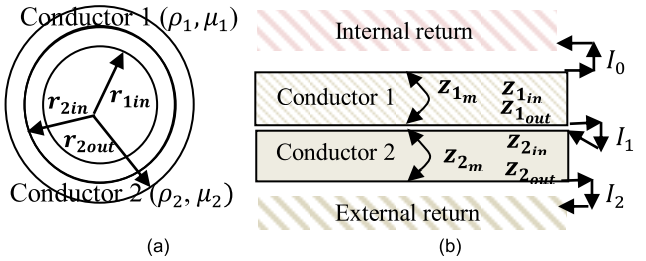

FIGURE 2. Circular & longitudinal cross section of a double layered conductor.

Z_{11} = The effective impedance of the inner surface of the whole double layered hollow tubular conductor with internal return.

Z_{22} = The effective impedance of the outer surface of the whole double layered hollow tubular conductor with external return.

$Z_{12} = Z_{21}$ = Mutual impedance between the conductor 1 and 2

These component impedances are determined here using Schelkunoff's theorems given by (1) and (2).

As per [23], each layer in a double layered conductor system, shown in Fig. 2 (b), can be treated as individual tubular conductor where $z_{1_{in}}$, $z_{1_{out}}$, z_{1_m} and $z_{2_{in}}$, $z_{2_{out}}$, z_{2_m} are respectively the inner surface, outer surface and mutual impedance of conductor 1 and 2 respectively, which are determined using (3) to (5).

a: EFFECTIVE OUTER SURFACE IMPEDANCE (Z_{22})

While determining effective outer surface impedance (Z_{22}) of the double layered conductor, the return path for all current is external as per the definition of Z_{22} given above. Therefore in Fig. 2 (b), internal return current, $I_0 = 0$, and total current of conductor 1 i.e. I_1 will return externally through the inner surface of the outermost layer i.e. conductor 2.

Now the electric field strength $\left(E_{z_{2i}}\right)$ along the conductor 2 inner surface can be derived from (1) and (2) as,

$$E_{z_{2i}} = -\Delta V = (I_2 z_{2_m} - I_1 z_{2_{in}}) \tag{7}$$

Also the longitudinal electric field remains continuous at the boundary between the outer and inner surface of the conductor 1 and conductor 2 respectively. Thus,

$$E_{z_{2i}} = E_{z_{1o}} = -\Delta V = I_1 z_{1_{out}} \tag{8}$$

where $E_{z_{1o}}$ is the longitudinal electric field along the outer surface of conductor 1.

If the electric field strength on conductor 2 outer surface is denoted by $E_{z_{2o}}$, it can be calculated as,

$E_{z_{2o}}$ = (Effective outer surface impedance of whole double layered conductor system, Z_{22}, multiplied with outer surface current,

$$I_2) = I_2 Z_{22} \tag{9}$$

While, as per (2) it can also be derived as,

$$E_{z_{2o}} = (I_2 z_{2_{out}} - I_1 z_{2_m}) \tag{10}$$

Solving (9) to (12) gives,

$$Z_{22} = (z_{2_{out}} - \frac{z_{2_m}^2}{z_{1_{out}} + z_{2_{in}}}) \tag{11}$$

b: EFFECTIVE INNER SURFACE IMPEDANCE (Z_{11}) AND MUTUAL IMPEDANCE BETWEEN INNER AND OUTER SURFACE (Z_{12})

As per the definition of Z_{11} given in the previous section, the return path for current in all layers outer to the conductor 1 is considered to be internal. Therefore in Fig. 2 (b), external return current, $I_2 = 0$ and the total current of conductor 2 returns internally through the outer surface of the innermost conductor i.e. conductor 1.

Now the electric field strength ($E_{z_{1o}}$) along the conductor 1 outer surface is obtained from (1) and (2) as,

$$E_{z_{1o}} = -\Delta V = (I_1 z_{1_{out}} - I_0 z_{1_m}) \tag{12}$$

But as the electric field is continuous at the boundary between the outer and inner surface of the conductor 1 and 2 respectively, it gives,

$$E_{z_{1o}} = E_{z_{2i}} = -\Delta V = (-I_1 z_{2_{in}}) \tag{13}$$

If the electric field strength on the conductor 1 inner surface is denoted by $E_{z_{1i}}$, it can be calculated as,

$E_{z_{1i}}$ = (Effective inner surface impedance of whole double layered conductor system , Z_{11}, multiplied with inner surface current,

$$I_0) = I_0 Z_{11} \tag{14}$$

While using (1) and (2), $E_{z_{1i}}$ will be obtained as,

$$E_{z_{1i}} = (I_1 z_{1_m} - I_0 z_{1_{in}}) \tag{15}$$

Thus solving (12) to (15), we get-

$$Z_{11} = (z_{1_{in}} - \frac{z_{1_m}^2}{z_{1_{out}} + z_{2_{in}}}) \tag{16}$$

So, (16) gives the effective impedance of inner surface of the whole double layered hollow tubular conductor.

Similarly, the mutual impedance between the conductor 1 and 2 can be derived as,

$$Z_{12} = \frac{z_{1_m} z_{2_m}}{z_{1_{out}} + z_{2_{in}}} \tag{17}$$

Therefore, (11), (16) and (17) give the effective outer surface, inner surface and mutual impedance of double layered coaxial conductor system respectively which will be applied to find out component impedances of conductor-semiconductor assembly present in the cable of Fig. 1. The cable has two such assemblies, such as core-semiconductor 1 and sheath-semiconductor 2 as shown in Fig. 1. Therefore following two cases are considered to find out the effective surface and mutual impedance of such assemblies present in the cable considered here.

Case I: Semiconductor 1 deposited on the core outer surface of the cable forms core-semiconductor 1 assembly, as shown in Fig. 1. In such assembly, when compared to the double layered conductor system of Fig. 2, core and semiconductor 1 correspond to conductor 1 and 2, respectively. The core-semiconductor 1 assembly has only the effective outer surface impedance ($Z_{con_1}^{sem_1}$) as the solid core is considered here, which can be determined using (11) as,

$$Z_{core}^{sem_1} = (\mathfrak{z}_{sem1_{out}} - \frac{\mathfrak{z}_{sem1_m}^2}{\mathfrak{z}_{coreout} + \mathfrak{z}_{sem1_{in}}}) \tag{18}$$

where, $\mathfrak{z}_{sem1_{out}}$, $\mathfrak{z}_{sem1_{in}}$ and $\mathfrak{z}_{sem1_m}$ are the inner & outer surface impedance and mutual impedance of semiconductor 1 respectively which can be determined using (3) to (5).

Case II: Another such assembly present in the cable of Fig. 1 is sheath-semiconductor 2 assembly which resembles a hollow double layered conductor system as depicted in Fig. 2 where sheath and semiconductor 2 corresponds to conductor 1 & 2 respectively. Being hollow this sheath-semiconductor 2 assembly has the following effective impedances derived from (11), (16) and (17) respectively,

Effective outer surface impedance,

$$Z_{sh_{out}}^{sem_2} = \mathfrak{z}_{sh_{out}} - \frac{\mathfrak{z}_{sh_m}^2}{\mathfrak{z}_{sem2_{out}} + \mathfrak{z}_{sh_{in}}} \tag{19}$$

Effective inner surface impedance,

$$Z_{sh_{in}}^{sem_2} = \mathfrak{z}_{sem2_{in}} - \frac{\mathfrak{z}_{sem2_m}^2}{\mathfrak{z}_{sem2_{out}} + \mathfrak{z}_{sh_{in}}} \tag{20}$$

Effective mutual impedance between the surfaces of the assembly,

$$Z_{sh_m}^{sem_2} = \frac{\mathfrak{z}_{sem2_m} \mathfrak{z}_{sh_m}}{\mathfrak{z}_{sem2_{out}} + \mathfrak{z}_{sh_{in}}} \tag{21}$$

where, $\mathfrak{z}_{sem2_{in}}$, $\mathfrak{z}_{sem2_{out}}$ and $\mathfrak{z}_{sem2_m}$ are the inner and outer surface impedance and mutual impedance of the semiconductor 2 respectively, which can be determined using (3) to (5).

When cable contains semiconductor on core only, it constitutes cable with single semiconducting screen whose loop impedance can be obtained by replacing $\mathfrak{z}_{core_{out}}$ in (6.*a*) with $Z_{core}^{sem_1}$. But when the semiconducting screen is attached with both core and sheath conductor, it constitutes cable with multiple semiconductors as shown in Fig. 1 whose loop impedances can be obtained by replacing surface and mutual impedance of core and sheath each in (4.a) to (4.c) with that of the core and sheath semiconductor assembly given by (19) to (21). So the loop impedances of cable with multiple semiconducting screens are given as,

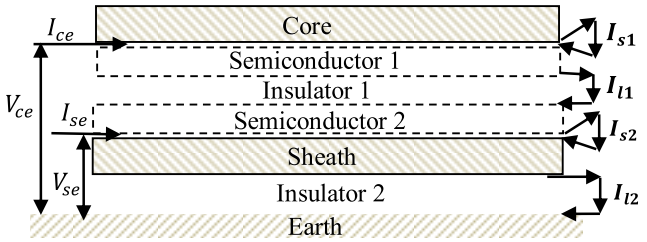

FIGURE 3. Loop & phase quantities in cable with multiple semiconducting screens.

$Z_{l_{11}}^{sem}$ = Self impedance of internal loop between core-semiconductor 1 and sheath-semiconductor 2 assembly

$$= Z_{core}^{sem_1} + \mathfrak{Z}_{ins_{12}} + Z_{sh_{in}}^{sem_2}$$
$$= \mathfrak{Z}_{sem_{1_{out}}} - \frac{\mathfrak{Z}_{sem_{1_m}}^2}{\mathfrak{Z}_{sem_{1_{out}}} + \mathfrak{Z}_{core_{out}}} + \mathfrak{Z}_{ins_{12}} + \mathfrak{Z}_{sem_{1_{out}}} - \frac{\mathfrak{Z}_{sem_{1_m}}^2}{\mathfrak{Z}_{sem_{1_{out}}} + \mathfrak{Z}_{sh_{in}}} \quad (22.a)$$

$Z_{l_{22}}^{sem}$ = Self impedance of the internal loop between sheath-semiconductor 2 assembly and earth

$$= Z_{sh_{out}}^{sem_2} + Z_e + \mathfrak{Z}_{ins_{2e}}$$
$$= \mathfrak{Z}_{sem_{2_{in}}} - \frac{\mathfrak{Z}_{sem_{2_m}}^2}{\mathfrak{Z}_{sem_{2_{out}}} + \mathfrak{Z}_{sh_{in}}} + Z_e + \mathfrak{Z}_{ins_{2e}} \quad (22.b)$$

$Z_{l_{12}}^{sem}$ = Mutual impedance between loop 1 and 2

$$= -\frac{\mathfrak{Z}_{sem_{2_m}} \mathfrak{Z}_{sh_m}}{\mathfrak{Z}_{sem_{2_{out}}} + \mathfrak{Z}_{sh_{in}}} \quad (22.c)$$

It is clear from the above expressions that the semiconducting screen influences the component impedance of only the conducting layer to which is attached.

Finally, the modified impedance matrix (Z_{mesh}^{sem}) of the cable with multiple semiconducting screens in mesh domain is given as,

$$[Z_{mesh}^{sem}] = \begin{bmatrix} Z_{l_{11}}^{sem} & Z_{l_{12}}^{sem} \\ Z_{l_{21}}^{sem} & Z_{l_{22}}^{sem} \end{bmatrix} \quad (23)$$

2) DERIVATION OF IMPEDANCE USING LOOP ANALYSIS

In this section, the expressions of impedance of the cable with multiple semiconducting screens obtained from the electromagnetic analysis, as discussed above, are reproduced using circuit analysis to show the robustness and accuracy of the adopted electromagnetic method. Fig. 3 shows that two local loops are formed between core-semiconductor 1 and sheath-semiconductor 2 assemblies. The loop voltages and loop currents are assumed to be ΔV_{l1}, ΔV_{l2} and I_{l1}, I_{l2} respectively. Also, two fictitious loops are considered between each conductor and its adjacent semiconducting screen where the loop voltages and currents are assumed to be ΔV_{s1}, ΔV_{s2} and I_{s1}, I_{s2} respectively, as shown in Fig. 3. Therefore the resulting loop equations for all the loops shown in Fig. 3 are as follows,

$$\Delta V_{s1} = I_{s1}\left(\mathfrak{Z}_{core_{out}} + \mathfrak{Z}_{sem_{1_{in}}}\right) - I_{l1}\mathfrak{Z}_{sem1_m} \quad (24.a)$$

$$\Delta V_{l1} = I_{l1}\left(\mathfrak{Z}_{sem_{1_{out}}} + \mathfrak{Z}_{sem_{2_{in}}} + \mathfrak{Z}_{ins_{12}}\right) - I_{s1}\mathfrak{Z}_{sem_{1_m}} - I_{s2}\mathfrak{Z}_{sem_{2_m}} \quad (24.b)$$

$$\Delta V_{s2} = I_{s2}\left(\mathfrak{Z}_{sem_{2_{out}}} + \mathfrak{Z}_{sh_{in}}\right) - I_{l1}\mathfrak{Z}_{sem_{2_m}} - I_{l2}\mathfrak{Z}_{sh_m} \quad (24.c)$$

$$\Delta V_{l2} = I_{l2}\left(\mathfrak{Z}_{sh_{out}} + \mathfrak{Z}_{ins_{2_e}} + Z_e\right) - I_{s2}\mathfrak{Z}_{sh_m} \quad (24.d)$$

But as the conductor and its conjugate semiconducting screen present in cable structure are at the same potential, $\Delta V_{s1} = \Delta V_{s2} = 0$ which when put in (24) and solve for ΔV_{l1} and ΔV_{l2}, yields the following,

$$\Delta V_{l1} = I_{l1}\left(\mathfrak{Z}_{sem_{1_{out}}} - \frac{\mathfrak{Z}_{sem_{1_m}}^2}{\mathfrak{Z}_{c_{2_{out}}} + \mathfrak{Z}_{sem_{1_{in}}}} + \mathfrak{Z}_{ins_{12}} + \mathfrak{Z}_{sem_{2_{in}}} - \frac{\mathfrak{Z}_{sem_{2_m}}^2}{\mathfrak{Z}_{sem_{2_{out}}} + \mathfrak{Z}_{sh_{in}}}\right) - I_{l2}\frac{\mathfrak{Z}_{sh_m}\mathfrak{Z}_{sem_{2_m}}}{(\mathfrak{Z}_{sem_{2_{out}}} + \mathfrak{Z}_{sh_{in}})} \quad (25.a)$$

$$\Delta V_{l2} = I_{l2}\left(\mathfrak{Z}_{sh_{out}} - \frac{\mathfrak{Z}_{sh_m}^2}{\mathfrak{Z}_{sh_{in}} + \mathfrak{Z}_{sem_{2_{out}}}} + \mathfrak{Z}_{ins_{12}} + Z_e\right) - I_{l1}\frac{\mathfrak{Z}_{sh_m}\mathfrak{Z}_{sem_{2_m}}}{(\mathfrak{Z}_{sem_{2_{out}}} + \mathfrak{Z}_{sh_{in}})} \quad (25.b)$$

So, the following self and mutual impedances of the cable with multiple semiconducting screens are obtained from (25.a) and (25.b),

Self impedance of internal loop between core-semiconductor 1 and sheath-semiconductor 2 assembly

$$= \mathfrak{Z}_{sem_{1_{out}}} - \frac{\mathfrak{Z}_{sem_{1_m}}^2}{\mathfrak{Z}_{sem_{1_{out}}} + \mathfrak{Z}_{core_{out}}} + \mathfrak{Z}_{ins_{12}} + \mathfrak{Z}_{sem_{1_{out}}} - \frac{\mathfrak{Z}_{sem_{1_m}}^2}{\mathfrak{Z}_{sem_{1_{out}}} + \mathfrak{Z}_{sh_{in}}} \quad (26.a)$$

Self impedance of the internal loop between sheath-semiconductor 2 assembly and earth

$$= \mathfrak{Z}_{sem_{2_{in}}} - \frac{\mathfrak{Z}_{sem_{2_m}}^2}{\mathfrak{Z}_{sem_{2_{out}}} + \mathfrak{Z}_{sh_{in}}} + Z_e + \mathfrak{Z}_{ins_{2e}} \quad (26.b)$$

Mutual impedance between loop 1 and 2

$$= -\frac{\mathfrak{Z}_{sem_{2_m}} \mathfrak{Z}_{sh_m}}{\mathfrak{Z}_{sem_{2_{out}}} + \mathfrak{Z}_{sh_{in}}} \quad (26.c)$$

It is clear that the impedance expressions of (26.a) to (26.c) obtained from circuit analysis matches exactly with the expressions of (22.a) to (22.c), obtained using the Schelkunoff's theory of tubular conductor, thus proving the robustness of the adopted electromagnetic method of finding the impedance of cable with multiple semiconducting screens.

D. IMPEDANCE OF CABLE IN PHASE DOMAIN

The relationships between voltage and current in the mesh domain of cable with multiple semiconducting screens are obtained from (25) as,

$$[V]_{mesh} = [I]_{mesh}[Z^{sem}_{mesh}] \tag{27}$$

where,

$$[V]_{mesh} = [\Delta V_{l1}\, \Delta V_{l2}]^T \tag{28}$$

$$[I]_{mesh} = [I_{l1}, I_{l2}]^T \tag{29}$$

and, $[Z^{sem}_{mesh}]$ is given by (23)

The current and voltage in different layers of cable measured w.r.t ground are known as phase current and voltage respectively, which are actually propagated through the practical cable. The phase currents and phase voltages of the cable considered here are I_{ce}, I_{se} and V_{ce}, V_{se} respectively as shown in Fig. 3.

The relationships between mesh quantities and phase quantities as obtained from Fig. 3 are, for current,

$$I_{l1} = I_{ce} \text{ and } I_{l2} = I_{ce} + I_{se} \tag{30}$$

for voltage,

$$\Delta V_{l1} = V_{ce} - V_{se} \text{ and } \Delta V_{l2} = V_{se} \tag{31}$$

Putting (30) and (31) in (27) gives,

$$\begin{bmatrix} V_{ce} - V_{se} \\ V_{se} \end{bmatrix} = \begin{bmatrix} I_{ce} \\ I_{ce} + I_{se} \end{bmatrix} [Z^{sem}_{mesh}] \tag{32}$$

Putting (23) on (32) and performing the row operations $R_1 \rightarrow R_1 + R_2$ on both sides of (32) and then multiplying and decomposing the quantities on LHS yields,

$$\begin{bmatrix} V_{ce} \\ V_{se} \end{bmatrix} = \begin{bmatrix} Z^{sem}_{l_{11}} + 2Z^{sem}_{l_{12}} + Z^{sem}_{l_{22}} & Z^{sem}_{l_{22}} + Z^{sem}_{l_{12}} \\ Z^{sem}_{l_{22}} + Z^{sem}_{l_{12}} & Z^{sem}_{l_{22}} \end{bmatrix} \begin{bmatrix} I_{ce} \\ I_{se} \end{bmatrix} \tag{33}$$

So, (33) gives the relationship between voltage and current in phase domain of cable with multiple semiconducting screens.

Here only the propagation through the central conductor is considered for analysis. Thus the self impedance of core-semiconductor assembly ($Z^{sem}_{Ph_{11}}$) is obtained from (33) as,

$$Z^{sem}_{Ph_{11}} = Z^{sem}_{l_{11}} + 2Z^{sem}_{l_{12}} + Z^{sem}_{l_{22}} \tag{34}$$

E. ADMITTANCE OF CABLE WITH SEMICONDUCTING SCREEN

As the propagation through the central conductor is considered for analysis here, the effective admittance between core and sheath $\left(Y_{e_{12}}\right)$ of the cable of Fig. 1 is determined as follows [24],

$$Y_{e_{12}} = \frac{1}{\frac{1}{y_{sem_1}} + \frac{1}{y_{ins_{12}}} + \frac{1}{y_{sem_2}}} = G_{e_{12}} + j\omega C_{e_{12}} \tag{35}$$

where $G_{e_{12}}$ and $C_{e_{12}}$ are the overall conductance and capacitance between the core and sheath semiconductor assembly of the cable.

TABLE 1. Parameters of 500 KV cable [25].

Cable Layer	Relative Permittivity	Resistivity (Ω-m)	Relative Permeability
Core Conductor	1.0	1.82×10^{-8}	1
Sheath Conductor	1.0	2.83×10^{-8}	1
Inner insulation	3.1	∞	0
Outer Insulation	4.0	∞	0
Semiconductor	Variable	variable	1

r_{ci}=0, r_{co}=30.45, r_{si}=71.15, r_{so}=74.8, r_{io}= 81.61, d=variable (*all dimensions are in mm*)

$\omega = 2\pi f; f$ = Frequency of propagated signal

y_{sem_i} = Admittance of i^{th} semiconducting screen where $i = 1$ & 2

$$= \frac{j\omega\varepsilon_0\varepsilon_{sem_i}}{\ln\frac{r_{out}}{r_{in}}} \;\&\; \varepsilon_{sem_i} = \varepsilon_{rsem_i} + \frac{1}{j\omega\rho_{sem_i}} \tag{36}$$

where ε_{rsem_i} and ρ_{sem_i} are the relative permittivity and resistivity of i^{th} semiconducting material respectively.

$y_{ins_{12}}$ = Admittance of insulating layer between core and sheath semiconductor assembly

$$= \frac{j\omega\varepsilon_0\varepsilon_{r_{ins_{12}}}}{\ln\frac{r_{out}}{r_{in}}} \text{ where } \varepsilon_{r_{ins_{12}}} = \varepsilon_r' - j\varepsilon_r'' \tag{37}$$

III. RESULT & DISCUSSION

All geometric and electromagnetic properties of a single core (SC) 500 kV cable containing semiconducting screen on core outer surface and sheath inner surface as shown in Fig.1, are furnished in Table. 1. A comparative analysis on the effects of different parameters of the semiconducting screen and frequency on line parameters and wave properties of the cable with single, multiple and no semiconducting screen are performed below.

A. CABLE PRIMARY LINE CONSTANTS

As the wave propagates through the cable in coaxial mode, it is governed by the self impedance ($Z^{sem}_{Ph_{11}}$) of core- semiconductor assembly and the effective admittance ($Y_{e_{12}}$) between core and sheath. Therefore the line parameters of the cable, namely resistive ($Re\ (Z^{sem}_{Ph_{11}})$) and inductive ($L^{sem}_{Ph_{11}}$) part obtained from $Z^{sem}_{Ph_{11}}$ and effective capacitance (C_e) obtained from Y_e are considered here for analysis.

1) VARIATION WITH SEMICONDUCTOR RESISTIVITY FOR DIFFERENT FREQUENCY

Fig. 4(a), (b) and (c) respectively show and compare the variation of Re ($Z^{sem}_{Ph_{11}}$), ($L^{sem}_{Ph_{11}}$) and $C_{e_{12}}$ with ρ_{sem} for different frequencies between the cable with multiple, single and without semiconducting screen. The semiconducting screen thickness (d) is kept fixed at 5 mm.

At low frequency, current mainly flows along the core conductor even when ρ_{sem} is in the range of conductor resistivity. Therefore, Re ($Z^{sem}_{Ph_{11}}$) of both the cable with single and multiple semiconducting screens has lower magnitude

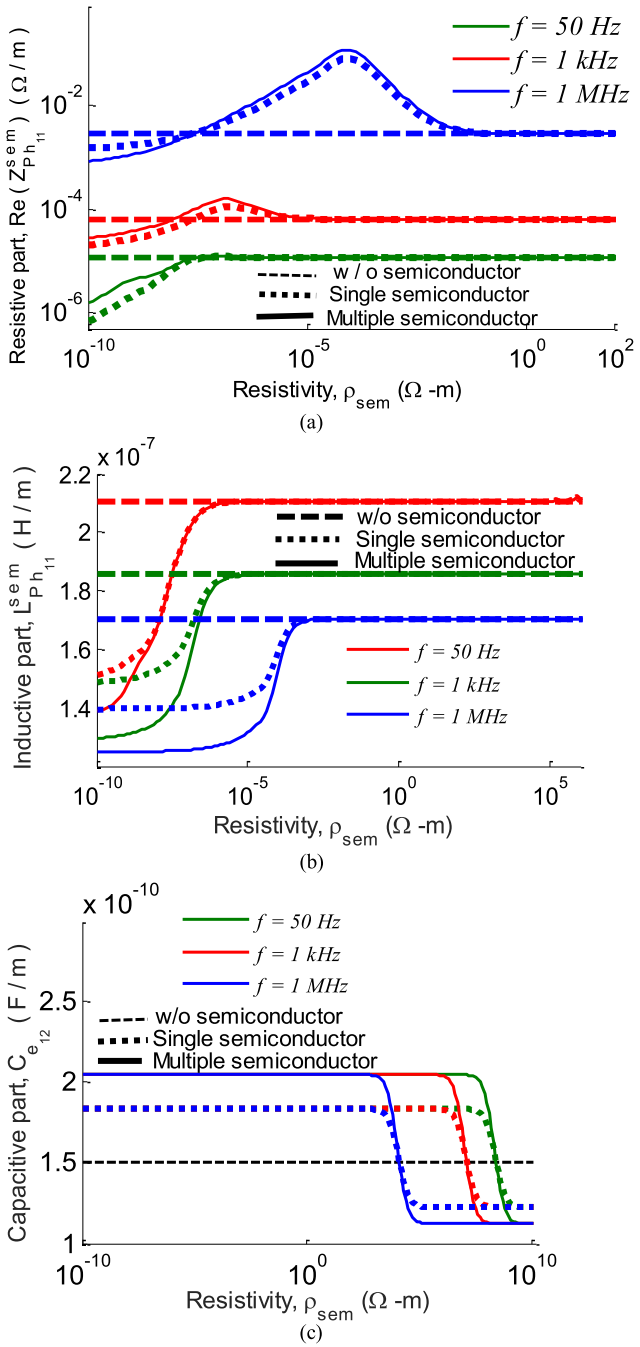

FIGURE 4. Variation with semiconductor resistivity for different frequency- (a) Resistive part, (b) Inductive part, (c) Capacitive part.

compared to that of the cable without semiconductor as shown in Fig. 4(*a*). But with the increase in frequency current redistributes towards the core surface due to skin effect and enters the semiconducting region. As a result, Re ($Z^{sem}_{Ph_{11}}$) of the cable with both single and multiple semiconducting screens is increasing with the increase of ρ_{sem} and reaches the maxima at a particular value of ρ_{sem} as shown in Fig. 4(a). Maxima of Re ($Z^{sem}_{Ph_{11}}$) of the cable with both single and multiple semiconducting screens occurs at the resistivity $1.973\times10^{-7}\Omega$- m and $1.973\times10^{-4}\Omega$- m for frequency 1 kHz and 1 MHz respectively as obtained from Fig. 4(a). When these resistivity values are put in the expression of skin depth (δ), given by,

$$\delta = \sqrt{\frac{\rho}{\omega\mu}} \tag{38}$$

skin depth (δ) comes out almost equal to 5 mm which is the thickness of the semiconducting screen. Thus it indicates that for a particular frequency, Re ($Z^{sem}_{Ph_{11}}$) reaches maxima at the value of ρ_{sem} for which skin depth becomes almost equal to the thickness of the semiconducting screen of the cable. More the frequency, more current flows in the semiconducting region. Thus higher resistivity is required to make skin depth equal to d. As a result, the value of ρ_{sem} at which peak of Re ($Z^{sem}_{Ph_{11}}$) occurs increases with the increase in frequency as shown in Fig. 4(a). With further increase of ρ_{sem}, the current redistribute towards the core from semiconducting region and resistance starts decreasing. When ρ_{sem} becomes much higher than the core resistivity, current mainly flows through the core even at high frequency and Re ($Z^{sem}_{Ph_{11}}$) settles to the value of the resistance provided by core alone, as seen in Fig. 4(*a*).

In case of a cable with multiple semiconducting screens, both core and sheath semiconducting screen contribute to the value of Re ($Z^{sem}_{Ph_{11}}$) at a higher frequency. As a result, both peak magnitude and rate of increase of Re ($Z^{sem}_{Ph_{11}}$) become higher in cable with multiple semiconducting screens compared to that of cable with single semiconducting screen, as seen in Fig. 4(a).

At a particular frequency, inductance of the cable without semiconductor is the maximum inductance at that frequency given by $\frac{\mu_0}{2\pi}\ln\frac{r_{si}}{r_{co}}$ as per Fig. 1 and its magnitude decreases with the increase in frequency as shown in Fig. 4(b). But at a particular frequency, when ρ_{sem} is lower than that of the conductor, most of the current use to flow along the core-semiconductor assembly's outer surface and sheath-semiconductor assembly's inner surface. Thus flux linkage takes place between the core-semiconductor assembly's outer and sheath's inner surface for cable with single semiconducting screen and between the core-semiconductor assembly's outer and sheath-semiconductor assembly's inner surface for cable with multiple semiconducting screens. Therefore, $L^{sem}_{Ph_{11}}$ is approximately given by $\frac{\mu_0}{2\pi}\ln\frac{r_{si}}{r_{co}+d}$ and $\frac{\mu_0}{2\pi}\ln\frac{r_{si}-d}{r_{co}+d}$ for cable with single and multiple semiconducting screens respectively where later has the lower magnitude as shown in Fig. 4(b). Also it is seen from Fig. 4(b) that the inductance of both the cable with single and multiple semiconducting screens is much lower than that of cable without semiconductor for this range of ρ_{sem}. But as ρ_{sem} starts increasing beyond this range, current migrates away from the surface of the semiconductor. As a result area of flux linkages is increasing which in turn increases the value of $L^{sem}_{Ph_{11}}$ and the difference between the value of $L^{sem}_{Ph_{11}}$ of the cable with single and multiple semiconducting screens is reducing as shown in Fig. 4(b). When ρ_{sem} increases to the value at which $\delta \approx d$ as per (39), axial current flows along the core outer surface and sheath inner surface. So, $L^{sem}_{Ph_{11}}$ of both the cable with single and multiple semiconducting screens reaches

the inductance of the cable without semiconductor at that frequency and remain fixed there with a further increase of ρ_{sem} as shown in Fig. 4(b). Also, higher the frequency, higher current resides in the semiconducting region. Thus higher ρ_{sem} is needed to make current returning to the conductor region. As a result, ρ_{sem} at which $L^{sem}_{Ph_{11}}$ reached the maximum value increases with the increase in frequency, as shown in Fig. 4(b).

At a particular frequency, when ρ_{sem} is lower than that of the conductor, charges are mainly accumulated on both side of the main insulator in both the cable with single and multiple semiconducting screens. As a result, $C_{e_{12}}$ of both the cable with single and multiple semiconducting screens remain fixed to the value approximately given by $\frac{2\pi\varepsilon_0\varepsilon_{ins_1}}{\ln\frac{r_{si}}{r_{co}+d}}$ and $\frac{2\pi\varepsilon_0\varepsilon_{ins_1}}{\ln\frac{r_{si}-d}{r_{co}+d}}$ respectively, as shown in Fig. 4(c). Clearly $C_{e_{12}}$ is more in cable with multiple semiconducting screens for this range of ρ_{sem} as seen in Fig. 4(c). With the increase of ρ_{sem} beyond this range, charges are moving towards the core and sheath conductor through the semiconducting region. Thus the effective capacitance of the cable now becomes a series combination of the capacitance of semiconducting and insulating layer which is always less than the capacitance provided by the insulating layer alone. As a result , $C_{e_{12}}$ is seen to be decreasing with ρ_{sem} in Fig. 4(c). When the value of ρ_{sem} becomes so high that charges mainly accumulate on core outer and sheath inner surface, $C_{e_{12}}$ becomes fixed to the lowest value equal to the effective capacitance between core outer and sheath inner surface of the cable as shown in Fig. 4(c). This value is lower in a cable with multiple semiconductors compared to that in a cable with single semiconductor as shown in Fig. 4(c) because in the former case, the capacitance is provided by the semiconducting screen of both core and sheath compared to that of the core alone in a cable with single semiconductor.

Also, higher the frequency, higher amount of charge resides in the semiconductor region and higher ρ_{sem} is required to send the charge from semiconducting to conducting region. As a result, higher the frequency, higher is the value of ρ_{sem} at which decrease in $C_{e_{12}}$ initiates as shown in Fig. 4(c).

The above discussions show that the inclusion of multiple semiconducting screens increases the resistive component of cable compared to that in the cable with single and no semiconducting screen. Also, for very low and high range of resistivity, semiconducting screen has minimal effect on the resistive component of the cable even at a very high frequency. It implies that the rate of attenuation can be increased considerably by including multiple semiconducting screens in cable structure especially at high frequency provided semiconductor resistivity is neither very high nor very low. On the other hand, inclusion of multiple semiconducting screens in cable structure reduces the inductive component but increases capacitance compared to the cable with single and no semiconducting screen. Thus it can be said that cable with multiple semiconductor may have a more significant influence on wave propagation velocity compared to that of the cable with single and no semiconducting screen.

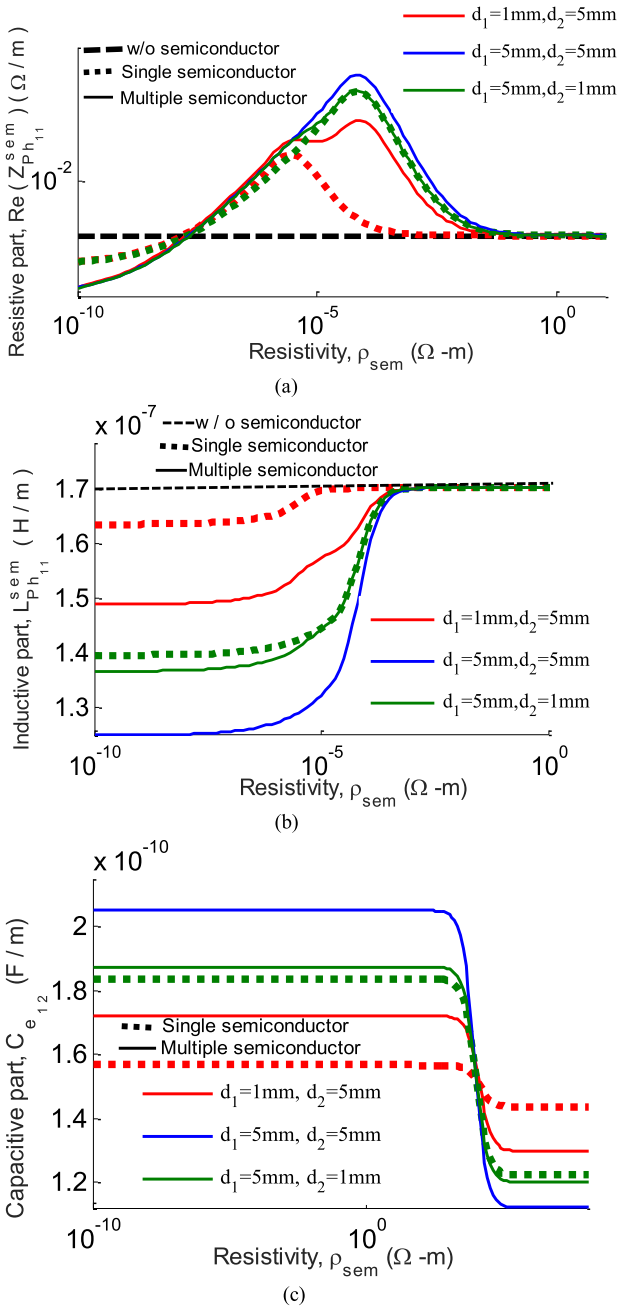

FIGURE 5. Variation with semiconductor resistivity for different thickness- (a) Resistive part, (b) Inductive part, (c) Capacitive part.

2) VARIATION WITH SEMICONDUCTOR RESISTIVITY FOR DIFFERENT THICKNESS

Fig. 5(a), (b) and (c) respectively show and compare the variation of Re $(Z^{sem}_{Ph_{11}})$, $L^{sem}_{Ph_{11}}$ and $C_{e_{12}}$ with ρ_{sem} between the cable with multiple, single and no semiconducting screen for different semiconducting screen thickness (d) keeping frequency fixed at 1 MHz. The maxima of Re $(Z^{sem}_{Ph_{11}})$ of the cable with single semiconducting screen takes place when

$\delta \approx d$ and δ increases with ρ_{sem} at a particular frequency as per (39). Therefore the resistivity at which peak of Re ($Z^{sem}_{Ph_{11}}$) of the cable with single semiconducting screen taken place increases with the increase in the thickness of semiconducting screen which in turn increases the overall Re ($Z^{sem}_{Ph_{11}}$) with the thickness, as shown in Fig. 5(a).

In case of a cable with multiple semiconducting screens, it is seen from Fig. 5(a) that when thickness (d_1) of core semiconductor is increasing from 1 to 5 mm by keeping sheath semiconductor thickness (d_2) fixed at 5 mm, Re ($Z^{sem}_{Ph_{11}}$) is also increasing for the same reason discussed above. When d_1 is kept fixed at 5 mm and d_2 is increasing from 1 to 5 mm, Re ($Z^{sem}_{Ph_{11}}$) is increasing, but the rate of increase is much lower compared to the former case. Also for smaller thickness of sheath semiconductor such as 1mm, peak takes place at lower resistivity which in turn reduces the contribution of sheath semiconductor in Re ($Z^{sem}_{Ph_{11}}$) significantly. As a result, Re ($Z^{sem}_{Ph_{11}}$) of cable with multiple semiconducting screens approaches to that of the cable with single semiconducting screen when the thickness of sheath semiconductor is quite small, as shown in Fig. 5(a). It is also seen from Fig. 5(a) that the resistivity at which peak of Re ($Z^{sem}_{Ph_{11}}$) of cable with multiple semiconducting screens taken place remains almost same irrespective of the thickness of sheath semiconductor.

At a particular frequency for low range of ρ_{sem}, $L^{sem}_{Ph_{11}}$ of cable with both single and multiple semiconducting screens is given by $\frac{\mu_0}{2\pi} \ln \frac{r_{si}}{r_{co}+d}$ and $\frac{\mu_0}{2\pi} \ln \frac{r_{si}-d}{r_{co}+d}$ respectively as shown previously. These expressions clearly show that when the thickness of the semiconducting screen (d) increases, $L^{sem}_{Ph_{11}}$ decreases and the rate of decrease is higher in a cable with multiple semiconducting screens as shown in Fig. 5(b). But with the increase of ρ_{sem}, $L^{sem}_{Ph_{11}}$ of both the cable with single and multiple semiconducting screens approaches the value of the inductance of cable without semiconductor at that frequency as discussed previously and thus the effect of semiconductor thickness on $L^{sem}_{Ph_{11}}$ will become negligible as shown in Fig. 5(b). It is also clear from Fig. 5(b) that sheath semiconductor has minimal effect on $L^{sem}_{Ph_{11}}$ when its thickness is quite low.

As discussed previously, at a particular frequency $C_{e_{12}}$ of both the cable with single and multiple semiconducting screens are approximately given by $\frac{2\pi\varepsilon_0\varepsilon_{ins_1}}{\ln \frac{r_{si}}{r_{co}+d}}$ and $\frac{2\pi\varepsilon_0\varepsilon_{ins_1}}{\ln \frac{r_{si}-d}{r_{co}+d}}$ respectively for lower range of ρ_{sem}. Thus for this range of ρ_{sem}, $C_{e_{12}}$ of both the cable with single and multiple semiconducting screens increases with the increase of the semiconductor thickness (d) and the latter has a higher rate of increase as shown in Fig. 5(c). But at a higher range of ρ_{sem}, $C_{e_{12}}$ becomes equivalent of the capacitance of semiconducting and insulating layer which is always less than the capacitance provided by the insulating layer alone. Now higher the value of d, lower will be the capacitance of the semiconducting screen, which in turn reduces $C_{e_{12}}$. Therefore at this higher range of ρ_{sem}, $C_{e_{12}}$ is decreasing with the increase of d for both the cable with single and multiple semiconductors as shown in Fig. 5(c). Also the cable with multiple semiconductors has lower $C_{e_{12}}$ as the capacitance is provided by the semiconducting screen of both core and sheath compared to that of the core alone in a cable with single semiconductor.

It can be said from the above discussions that the effect of semiconducting screen on all three line parameters of the cable becomes minimal for negligible screen thickness. Cable with multiple semiconducting screens has a higher rate and magnitude of change in all three line parameters with the increase in semiconductor thickness compared to the cable with single and no semiconducting screen. But the variation of line parameters of cable with multiple semiconducting screens approaches that of the cable with single semiconducting screens when the thickness of sheath semiconductor becomes minimal.

3) VARIATION WITH FREQUENCY FOR DIFFERENT SEMICONDUCTOR RESISTIVITY

Fig. 6(a), (b) and (c) show and compare the frequency variation of Re ($Z^{sem}_{Ph_{11}}$), $L^{sem}_{Ph_{11}}$ and $C_{e_{12}}$ respectively between the cable with single, multiple and no semiconducting screen for different ρ_{sem} keeping semiconductor thickness fixed at 5 mm. When the frequency is low, current mainly flows through core and sheath even when ρ_{sem} is quite low such as 1 mΩ - m. As a result, Re ($Z^{sem}_{Ph_{11}}$), $L^{sem}_{Ph_{11}}$ and $C_{e_{12}}$ of both the cable with single and multiple semiconducting screens have the same frequency variation as that of the cable without semiconductor as shown in Fig. 6. But with the increase of f, as current starts migrating away from the core, Re ($Z^{sem}_{Ph_{11}}$) starts increasing and when current enter semiconducting region there is a sudden rise in the value of Re ($Z^{sem}_{Ph_{11}}$) as shown in Fig. 6(a). The frequency at which the rise takes place is increasing with the increase of ρ_{sem} and cable with multiple semiconducting screens has almost 40% higher value of Re ($Z^{sem}_{Ph_{11}}$) than that in cable with single semiconducting screen as seen in Fig. 6(a) for the same reason discussed previously.

With the increase in f from low value, current starts migrating to semiconducting region and the area of flux linkage is reducing. As a result, $L^{sem}_{Ph_{11}}$ of both the cable with single and multiple semiconducting screens starts decreasing with the later has a higher rate of decrease as shown in Fig. 6(b). Also the frequency at which this decrease takes place increases with the increase of ρ_{sem} as seen in Fig. 6(b) for the same reason discussed above. Finally at very high frequency range, $L^{sem}_{Ph_{11}}$ of both the cable with single and multiple semiconducting screens become almost fixed to a much lower value than the inductance of cable without semiconductor as shown in Fig. 6(b). Also the inductance of cable with multiple semiconducting screens has the lowest value at this high frequency range.

For lower range of frequency, the axial current mainly flows through the core and sheath conductor. So, $C_{e_{12}}$ is determined as the series equivalent of capacitance between the core outer and sheath inner surface. Therefore for this

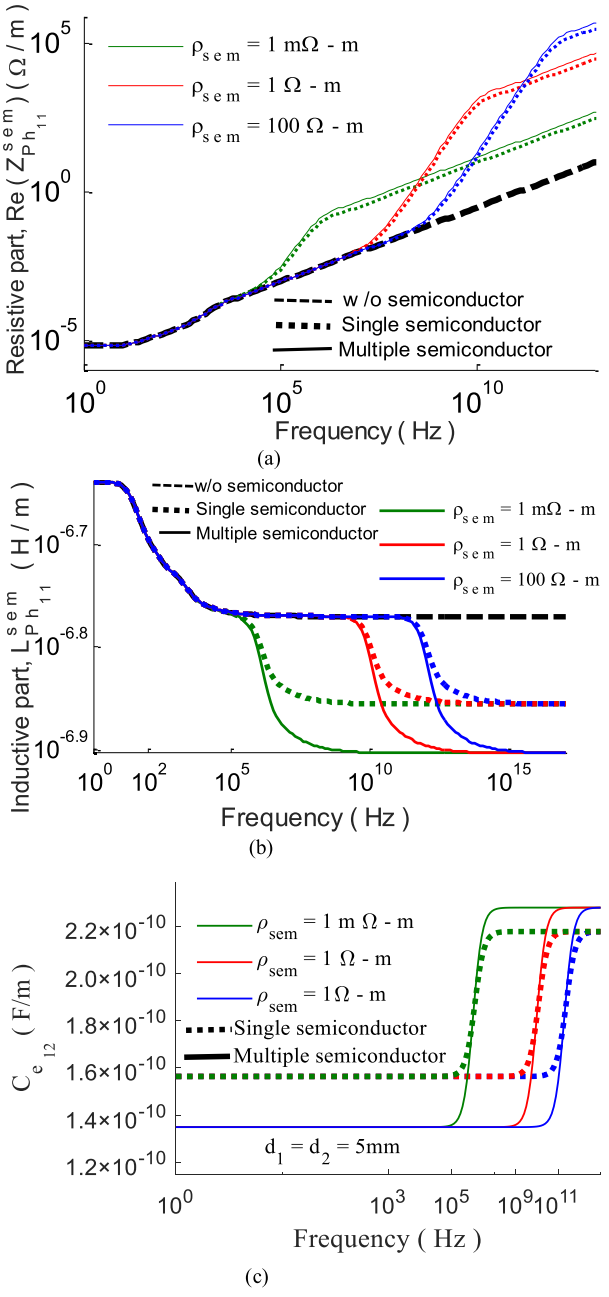

FIGURE 6. Variation with frequency for different semiconductor resistivity-(a) Resistive part, (b) Inductive part, (c) Capacitive part.

range of frequency, $C_{e_{12}}$ is higher in a cable with single semiconductor as shown in Fig. 6(c) as only core semiconductor is contributing to the value of $C_{e_{12}}$ compared to both core & sheath semiconductor in cable with multiple semiconducting screens. But with the increase in frequency, current migrates towards the core-semiconductor assembly's outer surface and sheath-semiconductor assembly's inner surface which increases the effective capacitance to the value provided by the insulating layer alone. As a result, $C_{e_{12}}$ in both the cable with single and multiple semiconducting screens increases to high value with cable with multiple semiconducting screens has higher magnitude as seen in Fig. 6(c).

The above discussions show that the effects of the semiconducting screen on cable line parameters come into play especially at high frequency region. Also these effects are enhanced with the inclusions of multiple semiconducting screens in cable structure compared to the cable with single and without semiconducting screen which in turn influences the wave propagation characteristics, especially at high frequency region.

B. WAVE PROPAGATION CHARACTERISTICS

Wave propagation characteristics of cable are determined by propagation constant (γ) which is the function of impedance (Z) and admittance (Y) of the cable, given by,

$$\gamma = \sqrt{ZY} = \alpha + j\beta \tag{39}$$

where α and β represent the attenuation constant and phase constant of the medium respectively. Here only coaxial mode of wave propagation is considered. Therefore the propagation constant is computed from the internal self impedance and admittance of the cable, given by (34) and (35) respectively. The variations of attenuation constant (α) and phase velocity (v_p) obtained from phase constant of cable with single, multiple and without semiconducting screen for different properties of semiconductor and frequency are discussed below.

1) ATTENUATION CONSTANT (α)

The real part of γ in (39), known as attenuation constant, is determined by the loss component of the cable. Thus α depends upon the resistive component of the cable and therefore influenced by the quantity and properties of the semiconducting screen in cable structure.

Fig. 7(a) and (b) show and compare the variation of α with ρ_{sem} respectively between the cable with single, multiple and no semiconducting screen for different frequency and thickness of the semiconducting screen. Both these variations of α resemble that of the resistive part of the cable depicted respectively in Fig. 4(a) and 5(a) as α is governed by the resistive part of the cable.

Just like Re ($Z^{sem}_{Ph_{11}}$), variation of α of both the cable with single and multiple semiconducting screens resembles with that of cable without semiconductor for very small and high range of ρ_{sem} at a particular frequency and thickness, as shown in Fig. 6(a) and (b). Also, with the increase of ρ_{sem} from very low value, α of both the cable with single and multiple semiconducting screens increases to reach the peak value and then decreases with a further increase in ρ_{sem}. The rate of attenuation increases with the increase in f as well as d similar to Re ($Z^{sem}_{Ph_{11}}$). Also higher the value of f and d, higher is the ρ_{sem} at which peak of α takes place as seen in Fig. 6(a) and (b) respectively for the same reason discussed previously for Re ($Z^{sem}_{Ph_{11}}$). Here also cable with multiple semiconducting screens has higher rate and magnitude of α compared to that in cable with single and no semiconducting screen. Attenuation characteristics of the cable with multiple semiconducting screens approach that of the cable with single semiconducting

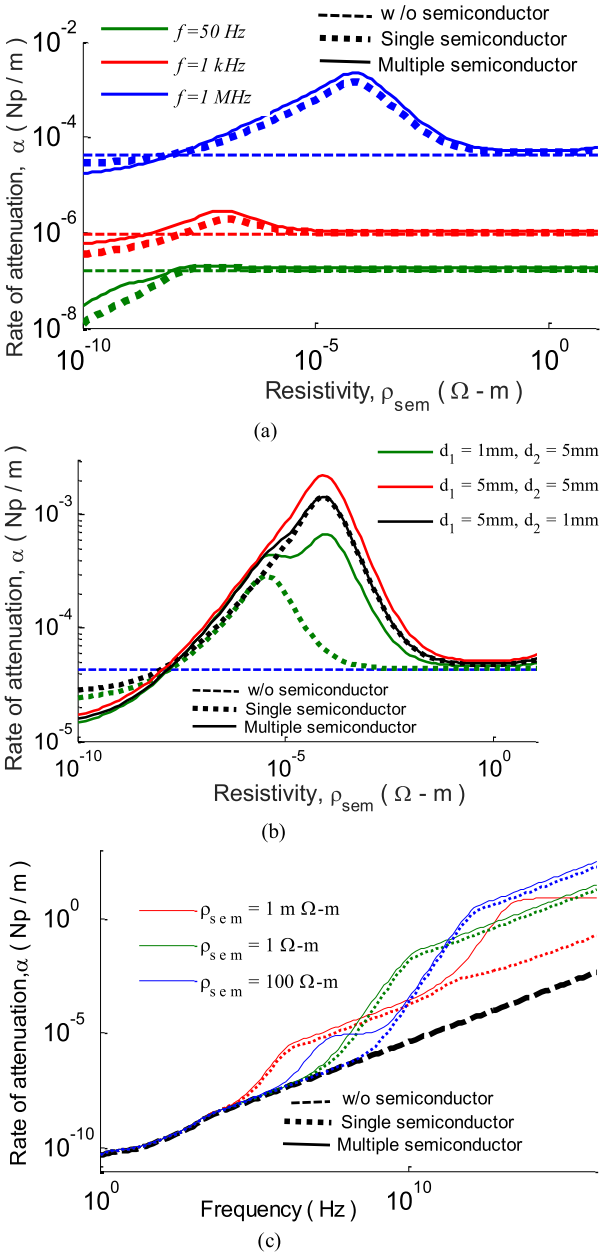

FIGURE 7. Variation of α–(a) with ρ_{sem} for different frequency, (b) with ρ_{sem} for different thickness, (c) with frequency for different ρ_{sem}.

screen when the thickness of sheath semiconductor becomes minimal as shown in Fig. 7(b).

The frequency variation of α for different ρ_{sem} depicted in Fig. 7(c) also resembles that of Re $(Z^{sem}_{Ph_{11}})$ shown in Fig. 6(a) for both cable with single and multiple semiconducting screens. Fig. 7(c) shows that like Re $(Z^{sem}_{Ph_{11}})$, α in a cable with semiconductor screen becomes higher with the increase of f compared to that in a cable without semiconductor after almost 100 kHz for the same reason mentioned in the previous section for Re $(Z^{sem}_{Ph_{11}})$. Also higher the ρ_{sem}, higher is the rate and magnitude of increase in α, especially at high frequency as shown in Fig. 7(c). Just like Re $(Z^{sem}_{Ph_{11}})$, cable with multiple semiconducting screens has higher rate and magnitude of increase in α compared to that in cable with single semiconducting screen.

2) PHASE VELOCITY (v_p)

The phase velocity (v_p) of the propagation can be determined from β in (38) as follows,

$$v_p = \frac{\omega}{\beta} \quad \text{where } \omega = 2\pi f \text{ and } f = \text{signal frequency}$$

As the phase of a signal is determined by the imaginary part of propagation constant, the phase velocity has an inverse relationship with inductive (L) and capacitive (C) part of the cable given by,

$$v_p = \frac{1}{\sqrt{LC}} \tag{40}$$

Therefore the quantity and properties of semiconducting screen present in cable structure influence v_p.

Fig. 8(a) shows the variation of v_p of the cable with single, multiple and no semiconducting screen with ρ_{sem} for different frequency. As discussed previously that at a very low range of ρ_{sem}, the variation of $L^{sem}_{Ph_{11}}$ and C_e has inverse nature of each other as given in Fig. 3(b) and (c) respectively. It makes v_p almost independent of semiconductor resistivity as per (39) even at high frequency as shown in Fig. 8(a). With the increase of ρ_{sem}, $L^{sem}_{Ph_{11}}$ starts increasing, but C_e remains constant at a high value. It results in a gradual decrease of v_p of both the cable with single and multiple semiconducting screens where the later has higher rate and magnitude of decrease. Beyond this resistivity range, $L^{sem}_{Ph_{11}}$ becomes almost fixed to the maximum value, whereas C_e is already constant to the high value. It makes v_p of both the cable to be fixed at a low value as shown in Fig. 8(a). However, at a very high range of ρ_{sem}, though $L^{sem}_{Ph_{11}}$ remains constant, C_e starts decreasing as seen in Fig. 3(c) which brings a sudden increase in v_p beyond the velocity of the cable without semiconducting screen, as shown in Fig. 7(a). For this range of ρ_{sem} also, the rate and magnitude of increase in v_p is higher in cable with multiple semiconducting screens.

It is shown in Fig. 7(b) that v_p of both the cable with single and multiple semiconducting screens remains almost independent of the variation of the thickness of semiconducting screen (d) for the very low range of ρ_{sem}. Because for this range of ρ_{sem}, the variation of $L^{sem}_{Ph_{11}}$ and C_e of the cable with d has inverse characteristics of each other as seen from Fig. 4(b) and (c) respectively. When ρ_{sem} increases beyond this range, both $L^{sem}_{Ph_{11}}$ and C_e of the cable with semiconducting screen are increasing with the increase in d and results in a gradual decrease in v_p with increasing d where the cable with multiple semiconducting screens has a higher rate of decrease as shown in Fig. 8(b). For very high range of ρ_{sem}, $L^{sem}_{Ph_{11}}$ becomes almost independent of d but C_e decreases with the increase in d. As a result, v_p of both the cable with single and multiple semiconductor increases with the increase in d beyond the velocity of the cable without semiconductor for this range of resistivity. Here also the cable with multiple

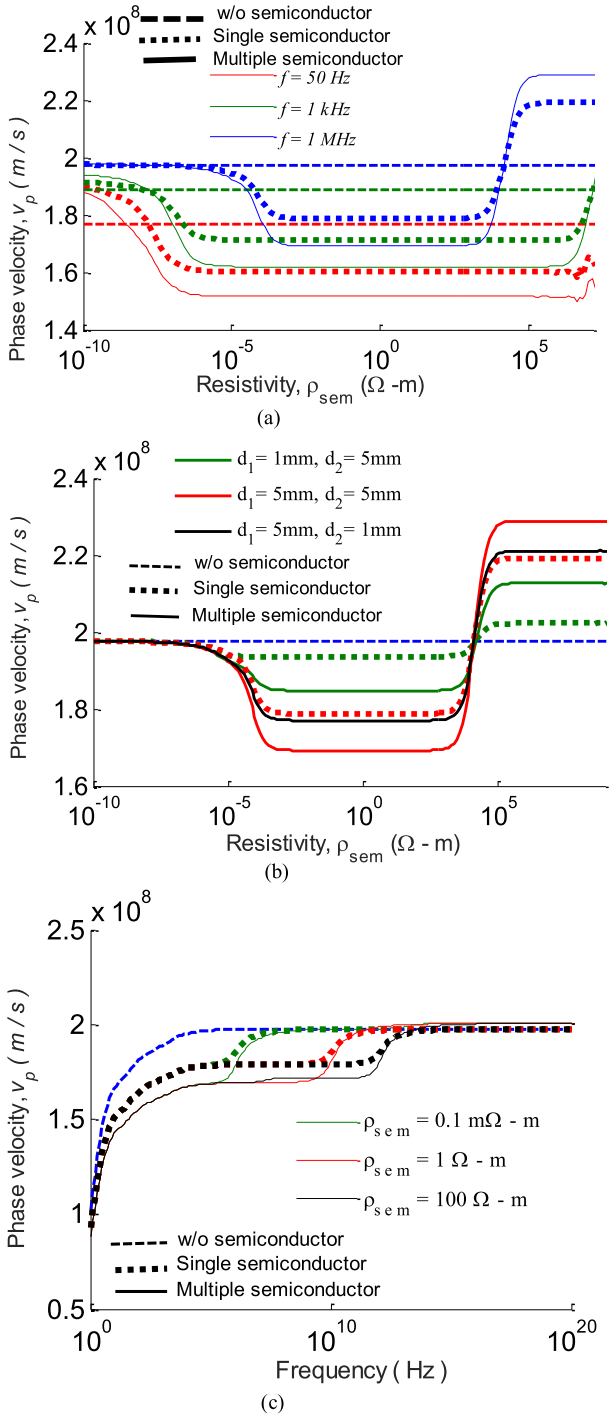

FIGURE 8. Variation of v_p – (a) with ρ_{sem} for different frequency, (b) with ρ_{sem} for different thickness, (c) with frequency for different ρ_{sem}.

semiconducting screens has higher rate and magnitude of increase compared to the cable with single semiconductor, as shown in Fig. 8(b).

Fig. 8(c) shows and compares the frequency variation of v_p between the cable with single, multiple and no semiconducting screen for different ρ_{sem}. It shows that there is no significant difference in v_p between the cable with and without semiconducting screen at a very low range of frequency as the semiconducting screen has a negligible effect on the inductive and capacitive part of the cable for this range of frequency as shown in Fig. 6(b) and (c). With the increase in frequency beyond this range, $L_{Ph_{11}}^{sem}$ and C_e of both the cable with single and multiple semiconductors tend to become constant respectively at a high and low value as shown in Fig. 6(b) and (c). As a result, cable with semiconducting screens has lower value of v_p compared to the cable without semiconductor as shown in Fig. 8(c). Also it is seen from the figure that the rate and magnitude of decrease in v_p are higher in the cable with multiple semiconductors. With further increase in frequency, $L_{Ph_{11}}^{sem}$ of the cable with both single and multiple semiconductors starts decreasing whereas C_e remains fixed to low value as shown in Fig. 6(b) and (c). As a result, v_p of both the cable with single and multiple semiconducting screens starts increasing at a higher rate to reach the velocity of the cable without semiconductor as shown in Fig. 7(c). It is seen from the figure that higher the value of ρ_{sem}, higher is the frequency at which this increase in v_p of the cable with semiconducting screen takes place. At very high frequency range, v_p of the cable with semiconducting screen is seen to cross the velocity of cable without semiconducting screen due to the very low value of $L_{Ph_{11}}^{sem}$.

So, the above discussions show that the wave propagation velocity is mainly governed by the inductive part of the cable for lower range of semiconductor resistivity whereas it becomes a function of mainly the capacitive part of the cable for high range of semiconductor resistivity especially at high frequency.

IV. CONCLUSION

In this paper the effects of inducting more than one semiconducting screen in cable structure on line parameters and wave properties of the cable are analyzed explicitly. Here the existing model of impedance of cable without semiconducting screen is modified using Schelkunoff's electromagnetic theory to include the effect of multiple semiconducting screens in the expressions of the cable impedance. The same expressions of impedance are reproduced using loop current method of network analysis to show the accuracy and robustness of the adopted electromagnetic approach. Based on the derived expressions of impedance and admittance, a comparative study on the effects of the variation of geometric and electromagnetic properties of the semiconducting screen on line parameters and wave properties of the cable with single, multiple and no semiconducting screen is performed to draw the following inferences,

1. The expressions of impedance of the cable with semiconducting screen reveal that the semiconducting screen influences the self and mutual impedance of that conducting layer only to which it is attached.

2. The effects of semiconducting screen on cable line parameters and wave properties become negligible for both very high and very low range of semiconductor resistivity. The same is also true when semiconductor thickness is minimal and signal frequency is low.

3. Inclusion of multiple semiconducting screens in cable structures increases the rate of attenuation compared to the cable with single and no semiconducting screen for a certain range of resistivity, especially at high frequency which is a desirable criterion for mitigating high frequency disturbances in cable. Also by increasing the thickness of semiconducting, screen attenuation can be increased but the thickness cannot be increased indefinitely due to mechanical constraint.

4. Wave propagation velocity in both the cable with single and multiple semiconducting screens is mainly governed by the inductive part of the cable for lower range of semiconductor resistivity and decreases considerably compared to the cable without semiconductor. The magnitude of velocity becomes lowest in the cable with multiple semiconductors for this range of resistivity. But for higher range of semiconductor resistivity, the wave propagation velocity in both the cable with single and multiple semiconducting screens almost becomes the function of the capacitive part only and increases beyond the value of the velocity in cable without semiconductor. Here also the magnitude of velocity is highest in the cable with multiple semiconductors for this range of resistivity.

So the inclusion of multiple semiconducting screens in cable structure has higher impact on wave properties of the cable compared to that in cable with single semiconductor and by varying different parameters of the semiconducting screen, the high frequency behavior of the cable can be improved.

REFERENCES

[1] L. M. Wedepohl, "Application of matrix methods to the solution of travelling-wave phenomena in polyphase systems," *Proc. Inst. Elect. Eng.*, vol. 110, no. 12, pp. 2200–2212, Dec. 1963, doi: 10.1049/piee.1963.0314.

[2] O. Breien and I. Johansen, "Attenuation of travelling waves in single-phase high-voltage cables," *Proc. Inst. Elect. Eng.*, vol. 118, no. 6, pp. 787–793, Jun. 1971, doi: 10.1049/piee.1971.0150.

[3] L. M. Wedepohl and D. J. Wilcox, "Transient analysis of underground power-transmission systems. System-model and wave-propagation characteristics," *Proc. Inst. Elect. Eng.*, vol. 120, no. 2, pp. 252–259, Feb. 1973, doi: 10.1049/piee.1973.0056.

[4] R. Schinzinger and A. Ametani, "Surge propagation characteristics of pipe enclosed underground cables," *IEEE Trans. Power App. Syst.*, vol. PAS-97, no. 5, pp. 1680–1688, Sep. 1978, doi: 10.1109/TPAS.1978.354660.

[5] A. Ametani, "A general formulation of impedance and admittance of cables," *IEEE Trans. Power App. Syst.*, vols. PAS–99, no. 3, pp. 902–910, May 1980, doi: 10.1109/TPAS.1980.319718.

[6] S. A. Schelkunoff, "The electromagnetic theory of coaxial transmission lines and cylindrical shields," *Bell Syst. Tech. J.*, vol. 13, no. 4, pp. 532–579, Oct. 1934.

[7] H. W. Dommel, *EMTP Theory Book*. Vancouver, BC, Canada: Microtran Power System Analysis, 1996.

[8] N. Nagaoka and A. Ametani, "A development of a generalized frequency-domain transient program-FTP," *IEEE Trans. Power Del.*, vol. 3, no. 4, pp. 1996–2004, Oct. 1988, doi: 10.1109/61.194010.

[9] A. Darcherif, A. Raizer, J. Sakellaris, and G. Meunier, "On the use of the surface impedance concept in shielded and multiconductor cable characterization by the finite element method," *IEEE Trans. Magn.*, vol. 28, no. 2, pp. 1446–1449, Mar. 1992, doi: 10.1109/20.123967.

[10] M. Kane, A. Ahmad, and P. Auriol, "Multiwire shielded cable parameter computation," *IEEE Trans. Magn.*, vol. 31, no. 3, pp. 1646–1649, May 1995, doi: 10.1109/20.376350.

[11] X. Liu, C. Ti, and G. Liang, "Wide-band modelling and transient analysis of the multi-conductor transmission lines system considering the frequency-dependent parameters based on the fractional calculus theory," *IET Gener., Transmiss. Distrib.*, vol. 10, no. 13, pp. 3374–3384, Oct. 2016, doi: 10.1049/iet-gtd.2016.0472.

[12] J. C. L. V. Silva, A. C. S. Lima, A. P. C. Magalhães, and M. T. C. de Barros, "Modelling seabed buried cables for electromagnetic transient analysis," *IET Gener., Transmiss. Distrib.*, vol. 11, no. 6, pp. 1575–1582, Apr. 2017, doi: 10.1049/iet-gtd.2016.1464.

[13] W. L. Weeks and Y. M. Diao, "Wave propagation characteristics in underground power cable," *IEEE Trans. Power App. Syst.*, vol. PAS-103, no. 10, pp. 2816–2826, Oct. 1984, doi: 10.1109/TPAS.1984.318279.

[14] S. Boggs, A. Pathak, and P. Walker, "Partial discharge. XXII. High frequency attenuation in shielded solid dielectric power cable and implications thereof for PD location," *IEEE Elect. Insul. Mag.*, vol. 12, no. 1, pp. 9–16, Jan./Feb. 1996, doi: 10.1109/57.484104.

[15] B. Gustavsen, "Panel session on data for modeling system transients insulated cables," in *Proc. IEEE Power Eng. Soc. Winter Meeting. Conf.*, Columbus, OH, USA, Jan./Feb. 2001, pp. 718–723, doi: 10.1109/PESW.2001.916943.

[16] G. Mugala, R. Eriksson, and U. Gafvert, "High frequency characterization of the semi-conducting screens of medium voltage XLPE cables," in *Proc. Annu. Rep. Conf. Elect. Insul. Dielectric Phenomena*, Cancún, Mexico, Oct. 2002, pp. 887–890, doi: 10.1109/CEIDP.2002.1048937.

[17] R. Heinrich, S. Bonisch, D. Pommerenke, R. Jobava, and W. Kalkner, "Broadband measurement of the conductivity and the permittivity of semiconducting materials in high voltage XLPE cables," in *Proc. 8th Int. Conference on Dielectric Mater., Meas. Appl.*, Edinburgh, U.K., Sep. 2000, pp. 212–217, doi: 10.1049/cp:20000507.

[18] S. Cristina and M. Feliziani, "A finite element technique for multiconductor cable parameters calculation," *IEEE Trans. Magn.*, vol. 25, no. 4, pp. 2986–2988, Jul. 1989, doi: 10.1109/20.34346.

[19] G. K. Papagiannis, D. G. Triantafyllidis, and D. P. Labridis, "A one-step finite element formulation for the modeling of single and double-circuit transmission lines," *IEEE Trans. Power Syst.*, vol. 15, no. 1, pp. 33–38, Feb. 2000, doi: 10.1109/59.852098.

[20] A. Ametani and K. Fuse, "Approximate method for calculating the impedances of multiconductors with cross sections of arbitrary shapes," *Elect. Eng. Jpn.*, vol. 112, no. 2, pp. 117–123, 1992, doi: 10.1002/eej.4391120213.

[21] R. A. Rivas and J. R. Marti, "Calculation of frequency-dependent parameters of power cables: Matrix partitioning techniques," *IEEE Trans. Power Del.*, vol. 17, no. 4, pp. 1085–1092, Oct. 2002, doi: 10.1109/TPWRD.2002.803827.

[22] P. D. Arizon and H. W. Dommel, "Computation of cable impedances based on subdivision of conductors," *IEEE Trans. Power Del.*, vol. 2, no. 1, pp. 21–27, Jan. 1987, doi: 10.1109/TPWRD.1987.4308068.

[23] N. Amekawa, A. Ametani, Y. Baba, and N. Nagaoka, "Derivation of a semiconducting layer impedance and its effect on wave propagation characteristics on a cable," *IEEE Trans. Power Del.*, vol. 19, no. 4, pp. 434–440, Jul. 2003, doi: 10.1049/ip-gtd:20030300.

[24] A. Ametani, Y. Miyamoto, and N. Nagaoka, "Semiconducting layer impedance and its effect on cable wave-propagation and transient characteristics," *IEEE Trans. Power Del.*, vol. 19, no. 4, pp. 1523–1531, Oct. 2004, doi: 10.1109/TPWRD.2003.822502.

[25] M. Hasheminezhad, M. Vakilian, T. R. Blackburn, and B. T. Phung, "Direct introduction of semicon layers in XLPE cable model," in *Proc. Int. Conf. Power Syst. Technol.*, Chongqing, China, Oct. 2006, pp. 1–7, doi: 10.1109/ICPST.2006.321520.

[26] G. Mugala, R. Eriksson, U. Gafvert, and P. Petterson, "Measurement technique for high frequency characterization of semiconducting materials in extruded cables," *IEEE Trans. Dielectr. Electr. Insul.*, vol. 11, no. 3, pp. 471–480, Jun. 2004, doi: 10.1109/TDEI.2004.1306725.

[27] G. Mugala, R. Eriksson, and P. Pettersson, "Comparing two measurement techniques for high frequency characterization of power cable semiconducting and insulating materials," *IEEE Trans. Dielectr. Electr. Insul.*, vol. 13, no. 4, pp. 712–716, Aug. 2006, doi: 10.1109/TDEI.2006.1667728.

[28] K. Steinbrich, "Influence of semiconducting layers on the attenuation behaviour of single-core power cables," *IEE Proc.—Gener., Transmiss. Distrib.*, vol. 152, no. 2, pp. 271–276, Mar. 2005, doi: 10.1049/ip-gtd:20050953.

[29] R. Paludo, G. C. da Silva, and V. S. Filho, "The study of semiconductor layer effect on underground cables with time domain reflectometry (TDR)," *IOSR J. Elect. Electron. Eng.*, vol. 7, no. 6, pp. 1–7, Sep./Oct. 2013, doi: 10.9790/1676-0760107.
[30] G. M. Hashmi, R. Papazyan, and M. Lehtonen, "Determining wave propagation characteristics of MVXLPE power cable using time domain reflectometrytechnique," *Turkish J. Elect. Eng. Comput. Sci.*, vol. 19, no. 2, pp. 207–219, 2011, doi: 10.3906/elk-1001-371.
[31] M. Tozzi, A. Cavallini, G. C. Montanari, and G. L. G. Burbui, "PD detection in extruded power cables: An approximate propagation mode," *IEEE Trans. Dielectr. Electr. Insul.*, vol. 15, no. 3, pp. 832–840, Jun. 2008, doi: 10.1109/TDEI.2008.4543121.
[32] M. Vakilian, T. R. Blackburn, R. E. James, and B. T. Phung, "Semiconducting layer as an attractive PD detection sensor of XLPE cables," *IEEE Trans. Dielectrics Electr. Insul.*, vol. 13, no. 4, pp. 885–891, Aug. 2006, doi: 10.1109/TDEI.2006.1667750.
[33] S. Gustafsson, T. Biro, G. Cinar, M. Gustafsson, A. Karlsson, B. Nilsson, S. Nordebo, and M. Sjöberg, "Electromagnetic dispersion modeling and measurements for HVDC power cables," *IEEE Trans. Power Del.*, vol. 29, no. 6, pp. 2439–2447, Dec. 2014, doi: 10.1109/TPWRD.2014.2324181.
[34] N. Okazima, Y. Baba, N. Nagaoka, A. Ametani, K. Temma, and T. Shimomura, "Propagation characteristics of power line communication signals along a power cable having semiconducting layers," *IEEE Trans. Electromagn. Compat.*, vol. 52, no. 3, pp. 756–769, Aug. 2010, doi: 10.1109/TEMC.2010.2046171.
[35] O. H. Nam, T. R. Blackburn, and B. T. Phung, "Modeling propagation characteristics of power cables with finite element techniques and ATP," in *Proc. Australas. Univ. Power Eng. Conf.*, Perth, WA, Australia, Dec. 2007, pp. 1–5, doi: 10.1109/AUPEC.2007.4548087.
[36] R. Papazyan, P. Pettersson, and D. Pommerenke, "Wave propagation on power cables with special regard to metallic screen design," *IEEE Trans. Dielectr. Electr. Insul.*, vol. 14, no. 2, pp. 409–416, Apr. 2007, doi: 10.1109/TDEI.2007.344621.
[37] W. Zhang, H.-J. Li, C. Liu, Y. Yang, Z. Huang, and R. Xue, "Parameter estimation technique for the semi-conducting layers in single-core XLPE cable," *IEEE Trans. Dielectr. Electr. Insul.*, vol. 21, no. 4, pp. 1916–1925, Aug. 2014, doi: 10.1109/TDEI.2014.004263.
[38] U. R. Patel and P. Triverio, "MoM-SO: A complete method for computing the impedance of cable systems including skin, proximity, and ground return effects," *IEEE Trans. Power Del.*, vol. 30, no. 5, pp. 2110–2118, Oct. 2015, doi: 10.1109/TPWRD.2014.2378594.
[39] Y. Li, P. A. A. F. Wouters, P. Wagenaars, P. C. J. M. van der Wielen, and E. F. Steennis, "Estimation of transmission line parameters single-core XLPE cables considering semiconducting layer," in *Proc. IEEE Int. Conf. Condition Monit. Diagnosis*, Bali, Indonesia, Sep. 2012, pp. 967–970, doi: 10.1109/CMD.2012.6416315.

SWARNANKUR GHOSH received the M.Tech. degree in electrical engineering from the Jalpaiguri Government Engineering College, Jalpaiguri, India, in 2012. He is currently pursuing the Ph.D. degree in electrical engineering from the National Institute of Technology Meghalaya, Meghalaya, India. His research interests include transients modeling of UG Cable, wave propagation through cable, and lightning transient.

MOUSAM GHOSH (M'16) received the B.Tech. degree in electrical engineering from the Jalpaiguri Government Engineering College, Jalpaiguri, India, in 2007, the M.E. degree in illumination engineering from the Electrical Engineering Department, Jadavpur University, Kolkata, India, in 2010, and the Ph.D. degree from the Maulana Abul Kalam Azad University of Technology (formerly known as West Bengal University of Technology), Nadia, India, in 2019.

He is currently an Assistant Professor with the Department of Electrical Engineering, Ramkrishna Mahato Government Engineering College, Purulia (formerly Purulia Government Engineering College), India. He was an Assistant Professor with the Department of Electrical Engineering, National Institute of Technology Meghalaya, Shillong, India. He is currently working on power electronics and drives. He has authored four numbers of the IEEE Transactions.

SUPRIYO DAS (M'09) received the master's degree from the Indian Institute of Technology Madras, India, in 2004, and the Ph.D. degree from the Indian Institute of Technology Kanpur, India, in 2014, both in electrical engineering. He is currently an Assistant Professor with the Department of Electrical Engineering, National Institute of Technology Meghalaya, India. His research interests include assessment and characterization of polymeric dielectrics, transient analysis, and lightning phenomena in electrical systems. He has authored two numbers of the IEEE Transactions.